Permanent diaphragmatic deficits and spontaneous respiratory plasticity in a mouse model of incomplete cervical spinal cord injury

Pauline Michel-Flutot, Arnaud Mansart, Thérèse B. Deramaudt, Isley Jesus, Kun Ze Lee, Marcel Bonay, Stéphane Vinit

Title: Permanent diaphragmatic deficits and spontaneous respiratory plasticity in a mouse model of incomplete cervical spinal cord injury

Authors and Affiliations:

Pauline Michel-Flutot[1], Arnaud Mansart[2], Therese B. Deramaudt[1], Isley De Jesus[1], Kun-Ze Lee[3], Marcel Bonay[1], Stéphane Vinit[1,*].

[1]Université Paris-Saclay, UVSQ, Inserm, END-ICAP, 78000 Versailles, France

[2] Université Paris-Saclay, UVSQ, Inserm, Infection et Inflammation (2I), 78000 Versailles, France

[3] Department of Biological Sciences, National Sun Yat-sen University, Kaohsiung, Taiwan

* Corresponding author:

Stéphane Vinit, PhD, HDR

Université Paris-Saclay, UVSQ, Inserm, END-ICAP, 78000 Versailles, France

E-mail: stephane.vinit@uvsq.fr

Phone: +33170429427

Abstract

High spinal cord injuries (SCI) lead to permanent respiratory insufficiency, and the search for new therapeutics to restore this function is essential. To date, the most documented preclinical model for high SCI is the rat cervical C2 hemisection. However, molecular studies with this SCI model are limited due to the poor availability of genetically modified specimens. The aim of this work was to evaluate the pathophysiology of respiratory activity following a cervical C2 injury at different times post-injury in a C57BL/6 mouse model. No significant spontaneous recovery of diaphragmatic activity was observed up to 30 days post-injury in eupneic condition. However, during a respiratory challenge, i.e. mild asphyxia, a partial restoration of the injured diaphragm was observed at 7 days post-injury, corresponding to the crossed phrenic phenomenon. Interestingly, the diaphragmatic recording between 2 respiratory bursts on the injured side showed an amplitude increase between 1 to 7 days post-injury, reflecting a change in phrenic motoneuronal excitability. This increase in inter-burst excitability returned to pre-injured values when the crossed phrenic phenomenon started to be effective at 7 days post-injury. Taken together, these results demonstrate the ability of the mouse respiratory system to express long-lasting plasticity following a C2 cervical hemisection and genetically modified animals can be used to study the pathophysiological effects on these plasticity phenomena.

Keywords

Mice; C2 spinal cord injury; Diaphragm EMG; Phrenic motoneuron

1. INTRODUCTION

High cervical spinal cord injuries (SCI) lead to neuromotor deficits, including respiratory insufficiency (Winslow and Rozovsky, 2003). For patients living with these deficits, mechanical ventilation is necessary for survival, and only a few of them may be weaned off ventilatory assistance. The development of new treatments aiming to ameliorate the living conditions of these patients is critical. A good preclinical model of respiratory insufficiency is *de facto* required to discover innovative efficient therapeutics that could be translated into clinics.

To date, the most studied pre-clinical model for evaluating putative therapeutics aimed to enhance respiratory function consists in doing a spinal cord injury at the cervical segment C2 in the rat. This model is the most documented in the field, especially the C2 hemisection (C2HS) model (Alilain et al., 2011; Golder et al., 2001; Goshgarian, 2003; Keomani et al., 2014; Lane et al., 2009; Lee et al., 2014; Nantwi et al., 1999; Porter, 1895; Vinit et al., 2006) or the C2 compression model (Nicaise et al., 2012; Wen et al., 2019; Wu M., 2019).

This highly reproducible model has demonstrated its usefulness in the study of several molecular pathways such as the respiratory motor plasticity by following daily acute intermittent hypoxia, which is mediated by modification in Brain-derived neurotrophic factor (BDNF) and Tropomyosin receptor kinase B (TrkB) expression (Lovett-Barr et al., 2012) or mTor/PTEN interaction (Gutierrez et al., 2013). Furthermore, the comprehension of a particular neuro-anatomical reorganization named the “crossed phrenic phenomenon” (CPP) (Goshgarian, 2003) following a cervical C2 injury still remains under investigation.

The descending respiratory pathways originate from the rostral ventral respiratory group located in the rostro-ventral medulla (Feldman et al., 2013). It connects bilaterally and monosynaptically to the phrenic motoneurons pool located between C3-C6 spinal segments

of the spinal cord in several species, such as human (Gandevia and Rothwell, 1987), cat (Feldman et al., 1985; Lipski et al., 1986), rat (Alexandrov et al., 2007) and more recently mouse (Vandeweerd et al., 2018). It also connects indirectly phrenic motoneurons via phrenic interneurons (Lane, 2011; Lane et al., 2008; Satkunendrarajah et al., 2018). The phrenic motoneurons project their axons through the phrenic nerves that innervate bilaterally the diaphragm, the main inspiratory muscle.

A unilateral C2HS induces a disruption of the bulbospinal tract from one side of the brainstem to the phrenic motoneurons innervating the diaphragm, leading to hemi-diaphragm paralysis. The contralateral side of the C2 hemi-injury remains intact, allowing the survival and recovery of the animal. In this model, a limited spontaneous recovery of the diaphragm activity can be observed over time post-injury. This recovery is sustained by the CPP, which consists in the activation of normally silent pathways crossing the spinal cord midline at the C3-C6 segmental level and connect to the ipsilateral deafferented phrenic motoneurons (Fuller et al., 2008; Vinit and Kastner, 2009). Strengthening the CPP pathways and providing new intraspinal connections to the deafferented motoneurons could be the substrate for developing new therapeutics in order to further improve the respiratory function following high SCI.

The rat model currently prevails for studying the effects of high cervical SCI because of its similarity to the human respiratory organization (Kastner and Gauthier, 2008). However, investigating the mechanistic approaches is limited in this model due to the poor availability of genetically modified specimens. Interestingly, the mouse model, with an extensive number of genetically modified strains can be used to decipher the molecular and cellular interactions. Mice are widely used in the study of the respiratory network (Cui et al., 2016; Wu et al., 2017; Zanella et al., 2014; Zholudeva et al., 2017) or several respiratory

pathologies such as Pompe disease (ElMallah et al., 2015) or Duchenne muscular dystrophy inducing diaphragm weakness (Burns et al., 2019). However, few studies used the mouse model of cervical injury to study post-traumatic spontaneous recovery and molecular pathophysiology (Mantilla et al., 2014; Minor et al., 2006; Nicaise et al., 2012; Satkunendrarajah et al., 2018). This emerging model needs further in depth investigation to better understand the spontaneous respiratory plasticity following cervical partial injury since the data pertaining to this mouse model are scarce (Streeter et al., 2019). In this study, we propose to evaluate the effect of a cervical spinal cord injury in C57BL/6 mouse strain on the diaphragm activity (eupnea and mild asphyxia) at different time points (up to one month post-injury). A better understanding of the functional effects resulting from such spinal injury could lead to a robust and reliable model for developing efficient therapeutics aimed to improve respiratory function.

2. MATERIAL AND METHODS

2.1. Ethics statement

All experiments reported in this manuscript were conformed to policies laid out by the National Institutes of Health (USA) in the Guide for the Care and Use of Laboratory Animals and EU Directive 2010/63/EU for animal experiments. These experiments were performed on adult C57BL/6 male and female mice (8-12 weeks old, Janvier, France). The animals were housed in individually ventilated cages in a state-of-the-art animal care facility (2CARE animal facility, accreditation A78-322-3, France), with access to food and water ad libitum on a 12 h light/dark cycle. These experiments were approved by the Ethics committee of the University of Versailles Saint-Quentin-en-Yvelines and complied with the French and European laws regarding animal experimentation (Apafis #8787-2017013115226134v4).

2.2. Chronic C2 hemisection

Animals were anesthetized with isoflurane (5% in 100% O_2) in a closed chamber. Anesthesia was maintained throughout the procedure (1.5-2% isoflurane in 100% O_2) through a nose cone. Animals were placed on a heating pad and the skin and muscles above the first vertebrae were retracted. A C2 laminectomy and a durotomy were performed. The spinal cord was ventro-laterally hemisected just caudal to the C2 dorsal roots by using micro-scissors followed by the use of a micro-scalpel to ensure the sectioning of all remaining fibers. The wounds and the skin were sutured closed. Sham mice underwent the same procedures without hemisection. The Isoflurane vaporizer was then turned off and mice received subcutaneous injections of analgesic (buprenorphine, 375 µg/kg: Buprecare from Axience) and antibiotics (40 mg/kg Trimethoprim and 200 mg/kg Sulfadoxin: Borgal 24%, from Virbac).

2.3. Electrophysiological recordings

A total of 72 animals were used for electrophysiological recordings. They were randomly and evenly (50% males, 50% females) divided into 12 different groups: 1h post-injury (P.I.) (n = 6) and 1h Sham (n = 6), 1d P.I. (n = 6) and 1d Sham (n = 6), 3d P.I. (n = 6) and 3d Sham (n = 6), 7d P.I. (n = 6) and 7d Sham (n = 6), 15d P.I. (n = 6) and 15d Sham (n = 6), 30d P.I. (n = 6) and 30d Sham (n = 6). At corresponding times post-injury, anesthesia was induced using 5% isoflurane in 100% O_2 and maintained throughout the experiment (2.5% in 21% O_2 balanced) through a nose cone. Animals were placed on a heating pad to maintain a physiological and constant body temperature. A laparotomy was performed to access the diaphragm. Both sides (ipsilateral and contralateral to the spinal cord lesion) of the diaphragm were tested for

their activity (electromyogram, EMG) using a handmade bipolar surface silver electrode on the mid-costal part of the muscle during spontaneous poïkilocapnic normoxic or transient mild asphyxia breathing (by occlusion of the animal nose for 15 s). EMGs were amplified (Model 1800; gain, 100; A-M Systems, Everett, WA, USA) and band pass-filtered (100 Hz to 10 kHz). The signals were digitized with an 8-channel Powerlab data acquisition device (Acquisition rate: 4 k/s; AD Instruments, Dunedin, New Zealand) connected to a computer and analyzed using LabChart 7 Pro software (AD Instruments, Dunedin, New Zealand). The bilateral diaphragmatic EMGs were integrated (50 ms decay). At the end of the experiment, animals were euthanized by intracardiac perfusion of heparinized 0.9% NaCl (10 mL) for tissue harvesting.

2.4. Histological reconstitution of the extent of C2 injury

The C1-C3 segment of the spinal cord was dissected out and immediately placed overnight in cold 4% paraformaldehyde, then cryoprotected for 48h in 30% sucrose (in 0.9% NaCl) and frozen. Longitudinal sections (30 µm thickness) were obtained with a Leica cryostat and the extent of injury was assessed after cresyl violet staining. . Slides were then scanned with an Aperio AT2 scanner (Leica, France) and a high resolution picture of each slide was taken to evaluate the extent of the injury and reported on a stereotaxic transverse plane (C2). Each injury was then digitized and analyzed with Image J software (NIH). The percentage of damaged tissue on the injured side was calculated by reference to a complete hemisection (which is 100% of the hemicord).

2.5. Data processing and statistical analyses

The amplitude (normalized to corresponding sham group in arbitrary units, AU) of minimally 5 double integrated diaphragm EMG inspiratory bursts during normoxia and mild asphyxia was calculated for each animal from the injured and the intact sides with LabChart 7 Pro software (AD Instruments). For inter-inspiratory bursts basal signal analysis during normoxia, the amplitude of minimal 5 basal diaphragmatic EMG signals were calculated, and the power spectral density (PSD) analysis was realized with LabChart 7, using a specific spectral setting (FFT size: 8K; Data window: Hamming; window overlap: 50%). At least, 5 windows of 35 ms were calculated for each side of each animal at all time points. For Sham animals, both left and right hemidiaphragm values were pooled together. Data were then gathered by boots of 100Hz for each animal and the mean for each group was calculated.

One-way ANOVA was performed between the different groups for the extent of injury evaluation or between the different post-lesioned time groups of the same condition. For diaphragmatic EMG, EMG inter-burst amplitude and PSD analysis, comparisons between intact and injured sides, and between eupnea and asphyxia were done by Student paired t-test. Comparisons between sham and injured animals were done by t-test. For PSD analysis, comparisons between frequency ranges and between times post-injury were done by a 2-way ANOVA (Tukey post hoc test).

All the data were presented as mean ± SEM and statistics were considered significant when $p<0.05$. SigmaPlot 12.5 software was used for all analyses.

3. RESULTS

3.1. Physiological effect

The body weight of animals did not show any significant variation over time following sham surgery. After C2 SCI, no statistical difference between injured animals with time post-injury

have been observed even if the animal's weight tends to be reduced up to 3d P.I. (initial weight = 22.8 ± 0.6 g *vs* 1d P.I. = 21.9 ± 0.6 g; 3d P.I. = 19.9 ± 0.7 g; 7d P.I. = 21.5 ± 0.7 g; 15d P.I. = 22.7 ± 1.4 g; 30d P.I. = 23.3 ± 1.3 g, One Way ANOVA, p=0.054). No difference in sham animals weight compared to injured animals (initial weight = 22.8 ± 0.5 g *vs* injured animals initial weight, p=0.834; 1d Sham = 21.1 ± 0.6 g *vs* 1d P.I., p=0.372; 3d Sham = 21.8 ± 0.9 g *vs* 3d P.I., p=0.092; 7d Sham 22.2 ± 0.8 g *vs* 7d P.I., p=0.513; 15d Sham = 22.3 ± 1.5 g *vs* 3d P.I., p=0.872; 30d Sham = 25.3 ± 1.9 g *vs* 3d P.I., p=0.413) at corresponding time post-surgery were observed (Table 1).

3.2. Effect on diaphragm activity during eupnea

No significant difference in injury size between all groups (1h P.I. = 91.4 ± 2.7 %; 1d P.I. = 90.6 ± 5.1 %; 3d P.I. = 86.1 ± 4.4 %; 7d P.I. = 85.5 ± 4.6 %; 15d P.I. = 94.3 ± 1.4 %; 30d P.I. = 94.4 ± 0.6 %; p = 0.248) was observed (Figure 1A, 1B and 1C). Diaphragmatic EMGs showed a significant decrease in diaphragm activity 1h after C2 injury (0.01 ± 0.01 A.U. *vs* Sham normalized to 1.00, p<0.001). This abolition persisted until 30d P.I. (1d P.I. = 0.04 ± 0.03 A.U. ; 3d P.I. = 0.03 ± 0.02 A.U. ; 7d P.I. = 0.22 ± 0.14 A.U. ; 15d P.I. = 0.19 ± 0.09 A.U. ; 30d P.I. = 0.30 ± 0.08 A.U.; *vs* Sham normalized to 1.00; p<0.001) on the injured side. At the intact side, diaphragm EMGs showed a significant increase at 1h P.I. (2.50 ± 0.38 A.U., p<0.001), 3d P.I. (1.48 ± 0.15 A.U. , p=0.006), 7d P.I. (1.62 ± 0.18 A.U. , p=0.002), 15d P.I. (2.76 ± 0.39 A.U. , p=0.001), 30d P.I. (1.93 ± 0.16 A.U. , p=0.002) but not at 1d P.I. (1.37 ± 0.47 A.U. , p=0.289) compared to the corresponding sham groups (normalized to 1.00 A.U.) (Figure 2A and 2B).

3.3. Diaphragm activity response to respiratory challenge

During mild asphyxia, all sham groups presented a significant increase in integrated diaphragm EMG amplitude compared to eupnea for all time points: 1h P.I. ($p<0.001$), 1d P.I. $p=0.003$), 3d P.I. ($p=0.012$), 7d P.I. ($p=0.002$), 15d P.I. ($p<0.001$) and 30d P.I. ($p<0.001$). For injured animals, the intact side did not show any significant variation in both conditions ($p>0.05$). At the injured side, a significant increase was observed at 7d P.I. ($p=0.031$), 15d P.I. ($p=0.002$) and 30d P.I. ($p=0.011$). No differences at 1h P.I., 1d P.I. and 3d P.I. ($p>0.05$) were observed (Table 2; Figure 3A to 3F).

3.4. Activity between respiratory bursts

Electrical recordings between EMG bursts and heart beats was analyzed (Figure 4A). A progressive increase in amplitude of the inter-burst activities at the injured side was observed over time, starting from 1d P.I. (injured side: 1d P.I. = 2.77 ± 0.99 A.U. *vs* Sham normalized to 1 $p=0.028$) and reaching a peak at 3d P.I. (injured side: 3d P.I. = 3.92 ± 0.97 A.U. *vs* 1h P.I. = 0.69 ± 0.12 A.U., $p=0.002$; 3d P.I. *vs* Sham normalized to 1, $p=0.002$; and 3d P.I. *vs* 1d P.I. = 2.77 ± 0.99 A.U., $p=0.048$). Then, the amplitude gradually decreased to pre-injury values at 7d P.I. (injured side: 2.49 ± 0.30 A.U. *vs* 3d P.I. $p=0.041$; *vs* Sham normalized to 1 $p<0.001$), 15d P.I. (injured side: 1.47 ± 0.28 A.U. *vs* 3d P.I., $p=0.002$; *vs* Sham normalized to 1 $p=0.008$) and 30d P.I. (injured side: 1.10 ± 0.09 A.U. *vs* 3d P.I., $p=0.002$; *vs* Sham normalized to 1 $p=0.248$). The intact side did not show any significant variation in inter-burst amplitude over time (intact side: 1h P.I. = 0.82 ± 0.15 A.U.; 3d P.I. = 1.17 ± 0.22 A.U.; 7d P.I. = 1.40 ± 0.27 A.U.; 15d P.I. = 1.09 ± 0.07 A.U.; 30d P.I. = 1.10 ± 0.07 A.U.; *vs* Sham normalized to 1 $p>0.05$), except at 1d P.I. (0.82 ± 0.15 A.U. vs Sham normalized to 1 $p=0.044$). Interestingly, at 3d P.I. the difference between the intact and the injured side was significant

(intact side vs injured side, p=0.042) and persisted until 7d P.I. (intact side vs injured side, p=0.029) (Figure 4B).

3.5. Power spectral density analysis

The PSD analysis of inter-burst recordings revealed an increase in low-end frequencies (from 100 to 1000Hz) at the injured side, similar to those observed during motor unit contraction (Supplemental data 1). For several range of frequencies, the number of events were significantly higher (1d P.I.: 200-300 Hz; 300-400 Hz; 400-500 Hz; 500-600 Hz; 600-700; *vs* 1hP.I.: 200-300 Hz, p=0.01; 300-400 Hz, p<0.001; 400-500 Hz, p=0.008; 500-600 Hz, p=0.008; 600-700 Hz p=0.002; Supplementary Table; Figure 5A-B). This increase was maintained at 3d P.I. for lower frequencies (3d P.I.: 200-300 Hz; 400-500 Hz; 500-600 Hz; 700-800 Hz; *vs* 1h P.I., p≤0.049; and *vs* 1d P.I., p>0.05; Supplementary Table; Figure 5C). At 7d P.I., most of the frequencies returned to pre-injury ones (1d P.I. *vs* 7d P.I.: 300-400 Hz, p<0.001; 600-700 Hz, p=0.018; 3d P.I. *vs* 7d P.I.: 400-500 Hz, p<0.001; 500-600 Hz, p=0.004; Supplementary Table; Figure 5D). For 15d P.I. and 30d P.I., the profiles obtained were similar to 1h P.I. and sham values (Supplementary Table and supplemental data 2). Interestingly, the observed profile correlated with the one obtained with the inter-burst signal amplitude analysis, with an increase observed between 1h P.I. and 3d P.I. A significant increase was also observed at 1d P.I. for the intact side compared to the other time points (1d P.I.: 100-200 Hz; 200-300 Hz; 300-400 Hz; *vs* 1h P.I.: 100-200 Hz, p=0.004; 200-300 Hz, p=0.002; 300-400 Hz, p<0.001; 1dP.I. *vs* 3d P.I.: 100-200 Hz, p=0.005; 200-300 Hz, p<0.001; 300-400 Hz, p<0.001; 1d P.I. *vs* 7d P.I.: 100-200 Hz, p=0.004; 200-300 Hz, p<0.001; 300-400 Hz, p<0.001; Supplementary Table; Figure 5A-D). Significant differences were also observed between intact and injured sides for some frequencies at 3d P.I. (intact side: 500-600 Hz; 600-700 Hz; 700-800 Hz; 800-

900 Hz; 900-1000 Hz; 1000-1100 Hz; *vs* injured side: 500-600 Hz; 600-700 Hz; 700-800 Hz; 800-900 Hz; 900-1000 Hz; 1000-1100 Hz, $p<0.04$; Supplementary Table; Figure 5C), as well as at 7d P.I. (intact side: 300-400 Hz; 500-600 Hz; 600-700 Hz; *vs* injured side: 300-400 Hz, $p=0.018$; 500-600 Hz, $p=0.039$; 600-700 Hz, $p=0.048$; Supplementary Table; Figure 5D).

4. DISCUSSION

The present study depicts for the first time the pathophysiology of the diaphragm muscle activity over time (up to one month P.I.) following a C2 cervical spinal cord injury in a mouse model.

The diaphragmatic activity of injured and sham mice was studied by surface EMG recordings in eupneic and mild asphyxic conditions in anesthetized animals. Under eupneic condition, the diaphragm activity did not show significant spontaneous recovery over time on the injured side. A non-significant increase in the integrated diaphragm EMG amplitude is observed from 7d P.I. to 30 d P.I., which could correspond to the occurrence of the spontaneous crossed phrenic phenomenon (Minor et al., 2006). In mice, following a C2HS injury, previous reports demonstrated the total annihilation of diaphragm activity up to 72h P.I. on the injured side (Minor et al., 2006). Interestingly, high cervical contusion injury at C4-C5 also induces a permanent diaphragm deficit which lasts up to 6 weeks P.I. (Nicaise et al., 2012). These present results are similar to those obtained in a rat model of C2HS (Goshgarian, 1981; Vinit et al., 2006). However, several publications have observed a robust spontaneous recovery of diaphragm activity in awake (Bezdudnaya et al., 2018; Sandhu et al., 2009) and even in anesthetized (Nantwi et al., 1999) rats. The discrepancy in these data is not unexpected since anesthetics, such as isoflurane used in this study, are known to induce a depression in the respiratory function (Teppema and Baby, 2011) and modulate respiratory

motoneurons and pre-motoneurons excitability (Stuth et al., 2008). However, these results showed that, even after a longer time point following injury, the mouse model may be a good model to study and test different therapeutics aimed to ameliorate the absence of respiratory function induced by cervical spinal injury.

As expected, during mild asphyxia, sham animals present a significant increase in diaphragm activity compared to eupneic condition at all time points post-sham surgery, which correlate with data seen in the literature (O'Halloran et al., 2002). The necessary increase in central respiratory drive during asphyxia, leads to a recruitment of additional diaphragmatic fibers and leads to an increase in diaphragm contraction. On the intact side of C2HS mice, the animals did not show any increase in diaphragm activity during asphyxia compared to eupneic conditions. This lack of increase could be due to a ceiling effect from the intact side, suggesting that the maximum drive on the uninjured hemidiaphragm during eupnea is at its optimal to counterbalance the absence of activity on the injured hemidiaphragm to maintain physiological values (Lee and Hsu, 2017). One strategy observed in C2HS animal models is the increase in respiratory frequency when animals are evaluated in awake eupneic condition (Dougherty et al., 2018), whereas in this case, no differences are observed in term of frequency (data not shown) since the animals are deeply anesthetized.

At the injured side, a mild asphyxia induces a significant diaphragmatic activity increase compared to eupnea at 7d, 15d and 30d P.I. This ability to further enhance the central spinal drive from the phrenic motoneurons to the diaphragm on the injured side can be sustained by the crossed phrenic pathways. These physical connections from the spared side of the spinal cord cross the midline at cervical level (C3-C6) and connect to the deafferented phrenic motoneurons. In certain conditions, these silent pathways can be spontaneously activated and lead to the activity resurgence on the injured side of the diaphragm

(Goshgarian, 2003; Minor et al., 2006; Moreno et al., 1992). This phenomenon, called the “crossed phrenic phenomenon”, has been described for the first time in 1895 by Porter on dogs and rabbits (Porter, 1895). By definition, this phenomenon induces an increase in the paralyzed hemidiaphragm and phrenic nerve activities following a spinal hemisection (above the level of phrenic motoneurons pools at cervical C2) with an additional contralateral phrenic nerve transection which strengthens the crossed pathways (Fuller et al., 2008; Lee et al., 2014; Vinit et al., 2006). Other conditions could increase the central respiratory drive and reveal the crossed phrenic phenomenon following C2HS, such as intermittent hypoxia (Golder and Mitchell, 2005), chronic intermittent hypoxia (Fuller et al., 2003) or asphyxia (Golder et al., 2003; O'Hara and Goshgarian, 1991). Here, these silent pathways are activated under mild asphyxic condition and lead to a partial activation of the paralyzed hemidiaphragm, similar to what has been previously observed in a rat model of C2HS (Golder et al., 2003; O'Hara and Goshgarian, 1991). In addition, the crossed pathways can be spontaneously activated over time post-C2 injury (Bezdudnaya et al., 2018; Fuller et al., 2008; Huang and Goshgarian, 2009).

The inter-burst signal between breaths and heart beats, named “noise signal”, was analyzed. Interestingly, a difference in basal noise value was observed with an amplitude increase at 1d P.I., 3d P.I., 7d P.I. and 15d P.I. with a maximum peak at 3d P.I. on the injured side. The intact side also showed a transient increase at 1d P.I. On the injured side, the decrease in signal amplitude observed between 3d P.I. and 15d P.I. could be due to the crossed phrenic pathway activation which starts to be observed at 7d P.I. Indeed, these previous silent pathways innervate deafferented phrenic motoneurons and can reactivate their bursting activity. The inter-burst signal on the injured side, corresponding to an increase in random deafferented unique spontaneous phrenic motoneuron activity, gradually increases until the

CPP strengthen its connections and re-innervate the deafferented phrenic motoneurons in order to resynchronize them and “stabilize” their own activity (Minor et al., 2006). Interestingly, phrenic motoneurons also receive inhibitory expiratory projections from the Bötzinger-complex expiratory neurons (Tian et al., 1998). Therefore, C2HS also interrupts this inhibitory bulbospinal pathway and could lead to a phrenic motoneuron disinhibition and then, induce spontaneous diaphragm EMG firing during the expiration phase. When the CPP (both inspiratory and expiratory pathways) occurs, the phrenic motoneurons are again inhibited by the Bötzinger-complex expiratory neurons and the inter-burst signal returns to pre-injured values. Another explanation could be a desynchronization of the phrenic motoneurons due to the injury (absence of bulbospinal rhythmic respiratory activity) between the different subtypes of phrenic motoneurons, i.e. early (early-I) and late (Late-I) inspiratory cells resulting in an increase of the inter-burst signal (Lee et al., 2013). Again, a resynchronization of every sub-types of phrenic motoneurons could be due to the occurrence of the CPP pathways. In addition, the power spectral density (PSD) of the inter-burst signal was analyzed in order to determine the physiological aspect of this signal. Indeed, power spectral analysis can be effectively used for fine analysis of muscle or nerve activities (ElMallah et al., 2016; Freund, 1983; Lindstrom and Magnusson, 1977). The range of frequencies observed in our inter-burst signal corresponds to those observed in diaphragmatic EMG PSD (see Supplemental data 1) and is similar to the one observed in rat diaphragmatic EMG (Seven et al., 2013). Taken altogether, our results demonstrate that the composition of this inter-burst signal at 3 d P.I. is similar to the composition of diaphragmatic EMG burst, i.e. corresponding to random phrenic motoneuron discharge. The spontaneous recovery from the CPP pathways re-synchronize the phrenic motoneurons together and leads to a modest functional recovery. Another explanation could be the venue

of a maladaptive behavior following central spinal injury. In fact, spasticity, which is a random contraction of skeletal muscle, is often observed following spinal injury in human (Kawamura et al., 1989; Sköld et al., 1999) and in rats (Bennett et al., 1999; Bennett et al., 2004; Li et al., 2004) and leads to serious motor dysfunction. Several mechanisms contribute to spasticity in rat following SCI, including a down-regulation of potassium-chloride cotransporter at the motoneurons membrane (Boulenguez et al., 2010) and a spontaneous activation of motoneuronal 5-HT_{2B} an 5-HT_{2C} receptors following injury (Murray et al., 2011). The spastic activity in our mice would occur faster compared to human and rat (Bennett et al., 1999). Nevertheless, this inter-burst activity disappears when rhythmic diaphragm EMG resolved at 7d P.I. One cannot rule out the massive inflammatory processes which can occur following cervical injury. Systemic inflammation can undermine subsequent respiratory plasticity and can impact the respiratory recovery following spinal injury (Hocker and Huxtable, 2019; Windelborn and Mitchell, 2012). More experiments will be needed in order to determine whether our diaphragm EMG recordings are spasms or a desynchronization of the phrenic motoneuronal activity.

5. CONCLUSION

Following C2HS, the diaphragmatic EMG did not reveal any significant spontaneous restoration of the respiratory function up to 30d P.I. in mice. However, the respiratory challenge (i.e. mild asphyxia) revealed the CPP at 7d P.I., demonstrating the tremendous plasticity of the bulbospinal descending respiratory pathways following high SCI. Interestingly, a change in the inter-burst signal of diaphragmatic EMG is observed between 1d P.I. and 7d P.I., which can be reversed by the emergence of the CPP. These findings show the ability of the mouse to be a robust model of respiratory impairment following C2HS,

opening new perspectives for the development of innovative therapeutics to reverse respiratory insufficiency.

Acknowledgements: This work was supported by funding from the Chancellerie des Universités de Paris (Legs Poix) (SV, MB), the Fondation de France (SV), the Fondation Médisite (SV), INSERM (MB, SV, AM), Université de Versailles Saint-Quentin-en-Yvelines (MB, SV, AM) and Ministry of Science and Technology 109-2636-B-110-001 (KZL). The supporters had no role in study design, data collection and analysis, decision to publish, or preparation of the manuscript.

Conflicts of interest: No conflict of interest

REFERENCES

Alexandrov, V.G., Ivanova, T.G., Alexandrova, N.P., 2007. Prefrontal control of respiration. J Physiol Pharmacol 58 Suppl 5, 17-23.

Alilain, W.J., Horn, K.P., Hu, H., Dick, T.E., Silver, J., 2011. Functional regeneration of respiratory pathways after spinal cord injury. Nature 475, 196-200.

Bennett, D.J., Gorassini, M., Fouad, K., Sanelli, L., Han, Y., Cheng, J., 1999. Spasticity in rats with sacral spinal cord injury. Journal of neurotrauma 16, 69-84.

Bennett, D.J., Sanelli, L., Cooke, C.L., Harvey, P.J., Gorassini, M.A., 2004. Spastic long-lasting reflexes in the awake rat after sacral spinal cord injury. J Neurophysiol 91, 2247-2258.

Bezdudnaya, T., Hormigo, K.M., Marchenko, V., Lane, M.A., 2018. Spontaneous respiratory plasticity following unilateral high cervical spinal cord injury in behaving rats. Experimental neurology 305, 56-65.

Boulenguez, P., Liabeuf, S., Bos, R., Bras, H., Jean-Xavier, C., Brocard, C., Stil, A., Darbon, P., Cattaert, D., Delpire, E., Marsala, M., Vinay, L., 2010. Down-regulation of the potassium-chloride cotransporter KCC2 contributes to spasticity after spinal cord injury. Nat Med 16, 302-307.

Burns, D.P., Drummond, S.E., Bolger, D., Coiscaud, A., Murphy, K.H., Edge, D., O'Halloran, K.D., 2019. N-acetylcysteine Decreases Fibrosis and Increases Force-Generating Capacity of mdx Diaphragm. Antioxidants (Basel) 8, E581.

Cui, Y., Kam, K., Sherman, D., Janczewski, W.A., Zheng, Y., Feldman, J.L., 2016. Defining preBötzinger Complex Rhythm- and Pattern-Generating Neural Microcircuits In Vivo. Neuron 91, 602-614.

Dougherty, B.J., Terada, J., Springborn, S.R., Vinit, S., MacFarlane, P.M., Mitchell, G.S., 2018. Daily acute intermittent hypoxia improves breathing function with acute and chronic spinal injury via distinct mechanisms. Respiratory physiology & neurobiology 256, 50-57.

ElMallah, M.K., Pagliardini, S., Turner, S.M., Cerreta, A.J., Falk, D.J., Byrne, B.J., Greer, J.J., Fuller, D.D., 2015. Stimulation of Respiratory Motor Output and Ventilation in a Murine Model of Pompe Disease by Ampakines. Am J Respir Cell Mol Biol 53, 326-335.

ElMallah, M.K., Stanley, D.A., Lee, K.-Z., Turner, S.M.F., Streeter, K.A., Baekey, D.M., Fuller, D.D., 2016. Power spectral analysis of hypoglossal nerve activity during intermittent hypoxia-induced long-term facilitation in mice. J Neurophysiol 115, 1372-1380.

Feldman, J.L., Del Negro, C.A., Gray, P.A., 2013. Understanding the rhythm of breathing: so near, yet so far. Annual review of physiology 75, 423-452.

Feldman, J.L., Loewy, A.D., Speck, D.F., 1985. Projections from the ventral respiratory group to phrenic and intercostal motoneurons in cat: an autoradiographic study. The Journal of neuroscience : the official journal of the Society for Neuroscience 5, 1993-2000.

Freund, H.J., 1983. Motor unit and muscle activity in voluntary motor control. Physiol Rev 63, 387-436.

Fuller, D.D., Doperalski, N.J., Dougherty, B.J., Sandhu, M.S., Bolser, D.C., Reier, P.J., 2008. Modest spontaneous recovery of ventilation following chronic high cervical hemisection in rats. Experimental neurology 211, 97-106.

Fuller, D.D., Johnson, S.M., Olson, E.B., Jr., Mitchell, G.S., 2003. Synaptic pathways to phrenic motoneurons are enhanced by chronic intermittent hypoxia after cervical spinal cord injury. The Journal of neuroscience : the official journal of the Society for Neuroscience 23, 2993-3000.

Gandevia, S.C., Rothwell, J.C., 1987. Activation of the human diaphragm from the motor cortex. J Physiol 384, 109-118.

Golder, F.J., Fuller, D.D., Davenport, P.W., Johnson, R.D., Reier, P.J., Bolser, D.C., 2003. Respiratory motor recovery after unilateral spinal cord injury: eliminating crossed phrenic activity decreases tidal volume and increases contralateral respiratory motor output. The Journal of neuroscience : the official journal of the Society for Neuroscience 23, 2494-2501.

Golder, F.J., Mitchell, G.S., 2005. Spinal synaptic enhancement with acute intermittent hypoxia improves respiratory function after chronic cervical spinal cord injury. The Journal of neuroscience : the official journal of the Society for Neuroscience 25, 2925-2932.
Golder, F.J., Reier, P.J., Bolser, D.C., 2001. Altered respiratory motor drive after spinal cord injury: Supraspinal and bilateral effects of a unilateral lesion. Journal of Neuroscience 21, 8680-8689.
Goshgarian, H.G., 1981. The role of cervical afferent nerve fiber inhibition of the crossed phrenic phenomenon. Experimental neurology 72, 211-225.
Goshgarian, H.G., 2003. Invited Review: The crossed phrenic phenomenon: a model for plasticity in the respiratory pathways following spinal cord injury. Journal of Applied Physiology 94, 795-810.
Gutierrez, D.V., Clark, M., Nwanna, O., Alilain, W.J., 2013. Intermittent hypoxia training after C2 hemisection modifies the expression of PTEN and mTOR. Experimental neurology 248, 45-52.
Hocker, A.D., Huxtable, A.G., 2019. Viral Mimetic-Induced Inflammation Abolishes Q-Pathway, but Not S-Pathway, Respiratory Motor Plasticity in Adult Rats. Front Physiol 10, 1039-1039.
Huang, Y., Goshgarian, H.G., 2009. Identification of the neural pathway underlying spontaneous crossed phrenic activity in neonatal rats. Neuroscience 163, 1109-1118.
Kastner, A., Gauthier, P., 2008. Are rodents an appropriate pre-clinical model for treating spinal cord injury? Examples from the respiratory system. Experimental neurology 213, 249-256.
Kawamura, J., Ise, M., Tagami, M., 1989. The clinical features of spasms in patients with a cervical cord injury. Paraplegia 27, 222-226.
Keomani, E., Deramaudt, T.B., Petitjean, M., Bonay, M., Lofaso, F., Vinit, S., 2014. A murine model of cervical spinal cord injury to study post-lesional respiratory neuroplasticity. J Vis Exp.
Lane, M.A., 2011. Spinal respiratory motoneurons and interneurons. Respiratory physiology & neurobiology 179, 3-13.
Lane, M.A., Lee, K.-Z., Fuller, D.D., Reier, P.J., 2009. Spinal circuitry and respiratory recovery following spinal cord injury. Respiratory physiology & neurobiology 169, 123-132.
Lane, M.A., White, T.E., Coutts, M.A., Jones, A.L., Sandhu, M.S., Bloom, D.C., Bolser, D.C., Yates, B.J., Fuller, D.D., Reier, P.J., 2008. Cervical prephrenic interneurons in the normal and lesioned spinal cord of the adult rat. Journal of Comparative Neurology 511, 692-709.
Lee, K.-Z., Dougherty, B.J., Sandhu, M.S., Lane, M.A., Reier, P.J., Fuller, D.D., 2013. Phrenic motoneuron discharge patterns following chronic cervical spinal cord injury. Experimental neurology 249, 20-32.
Lee, K.Z., Hsu, S.H., 2017. Compensatory Function of the Diaphragm after High Cervical Hemisection in the Rat. J Neurotrauma 34, 2634-2644.
Lee, K.Z., Huang, Y.J., Tsai, I.L., 2014. Respiratory motor outputs following unilateral midcervical spinal cord injury in the adult rat. J Appl Physiol (1985) 116, 395-405.
Li, Y., Gorassini, M.A., Bennett, D.J., 2004. Role of persistent sodium and calcium currents in motoneuron firing and spasticity in chronic spinal rats. J Neurophysiol 91, 767-783.
Lindstrom, L.H., Magnusson, R.I., 1977. Interpretation of myoelectric power spectra: A model and its applications. Proceedings of the IEEE 65, 653-662.
Lipski, J., Bektas, A., Porter, R., 1986. Short latency inputs to phrenic motoneurones from the sensorimotor cortex in the cat. Exp Brain Res 61, 280-290.
Lovett-Barr, M.R., Satriotomo, I., Muir, G.D., Wilkerson, J.E., Hoffman, M.S., Vinit, S., Mitchell, G.S., 2012. Repetitive intermittent hypoxia induces respiratory and somatic motor recovery after chronic cervical spinal injury. The Journal of neuroscience : the official journal of the Society for Neuroscience 32, 3591-3600.
Mantilla, C.B., Greising, S.M., Stowe, J.M., Zhan, W.-Z., Sieck, G.C., 2014. TrkB kinase activity is critical for recovery of respiratory function after cervical spinal cord hemisection. Experimental neurology 261, 190-195.
Minor, K.H., Akison, L.K., Goshgarian, H.G., Seeds, N.W., 2006. Spinal cord injury-induced plasticity in the mouse--the crossed phrenic phenomenon. Experimental neurology 200, 486-495.

Moreno, D.E., Yu, X.J., Goshgarian, H.G., 1992. Identification of the axon pathways which mediate functional recovery of a paralyzed hemidiaphragm following spinal cord hemisection in the adult rat. Experimental neurology 116, 219-228.
Murray, K.C., Stephens, M.J., Ballou, E.W., Heckman, C.J., Bennett, D.J., 2011. Motoneuron excitability and muscle spasms are regulated by 5-HT2B and 5-HT2C receptor activity. J Neurophysiol 105, 731-748.
Nantwi, K.D., El-Bohy, A.A., Schrimsher, G.W., Reier, P.J., Goshgarian, H.G., 1999. Spontaneous Functional Recovery in a Paralyzed Hemidiaphragm Following Upper Cervical Spinal Cord Injury in Adult Rats. Neurorehabilitation and Neural Repair 13, 225-234.
Nicaise, C., Putatunda, R., Hala, T.J., Regan, K.A., Frank, D.M., Brion, J.-P., Leroy, K., Pochet, R., Wright, M.C., Lepore, A.C., 2012. Degeneration of phrenic motor neurons induces long-term diaphragm deficits following mid-cervical spinal contusion in mice. Journal of neurotrauma 29, 2748-2760.
O'Halloran, K.D., McGuire, M., O'Hare, T., Bradford, A., 2002. Chronic intermittent asphyxia impairs rat upper airway muscle responses to acute hypoxia and asphyxia. Chest 122, 269-275.
O'Hara, T.E., Jr., Goshgarian, H.G., 1991. Quantitative assessment of phrenic nerve functional recovery mediated by the crossed phrenic reflex at various time intervals after spinal cord injury. Experimental neurology 111, 244-250.
Porter, W.T., 1895. The Path of the Respiratory Impulse from the Bulb to the Phrenic Nuclei. J Physiol 17, 455-485.
Sandhu, M.S., Dougherty, B.J., Lane, M.A., Bolser, D.C., Kirkwood, P.A., Reier, P.J., Fuller, D.D., 2009. Respiratory recovery following high cervical hemisection. Respiratory physiology & neurobiology 169, 94-101.
Satkunendrarajah, K., Karadimas, S.K., Laliberte, A.M., Montandon, G., Fehlings, M.G., 2018. Cervical excitatory neurons sustain breathing after spinal cord injury. Nature 562, 419-422.
Seven, Y.B., Mantilla, C.B., Zhan, W.-Z., Sieck, G.C., 2013. Non-stationarity and power spectral shifts in EMG activity reflect motor unit recruitment in rat diaphragm muscle. Respiratory physiology & neurobiology 185, 400-409.
Sköld, C., Levi, R., Seiger, A., 1999. Spasticity after traumatic spinal cord injury: nature, severity, and location. Archives of physical medicine and rehabilitation 80, 1548-1557.
Streeter, K.A., Sunshine, M.D., Brant, J.O., Sandoval, A.G.W., Maden, M., Fuller, D.D., 2019. Molecular and histologic outcomes following spinal cord injury in spiny mice, Acomys cahirinus. J Comp Neurol, 10.1002/cne.24836.
Stuth, E.A., Stucke, A.G., Brandes, I.F., Zuperku, E.J., 2008. Anesthetic effects on synaptic transmission and gain control in respiratory control. Respiratory physiology & neurobiology 164, 151-159.
Teppema, L.J., Baby, S., 2011. Anesthetics and control of breathing. Respiratory physiology & neurobiology 177, 80-92.
Tian, G.F., Peever, J.H., Duffin, J., 1998. Bötzinger-complex expiratory neurons monosynaptically inhibit phrenic motoneurons in the decerebrate rat. Experimental brain research 122, 149-156.
Vandeweerd, J.-M., Hontoir, F., De Knoop, A., De Swert, K., Nicaise, C., 2018. Retrograde Neuroanatomical Tracing of Phrenic Motor Neurons in Mice. J Vis Exp, 56758.
Vinit, S., Gauthier, P., Stamegna, J.C., Kastner, A., 2006. High cervical lateral spinal cord injury results in long-term ipsilateral hemidiaphragm paralysis. Journal of neurotrauma 23, 1137-1146.
Vinit, S., Kastner, A., 2009. Descending bulbospinal pathways and recovery of respiratory motor function following spinal cord injury. Respiratory physiology & neurobiology 169, 115-122.
Wen, M.-H., Wu, M.-J., Vinit, S., Lee, K.-Z., 2019. Modulation of Serotonin and Adenosine 2A Receptors on Intermittent Hypoxia-Induced Respiratory Recovery following Mid-Cervical Contusion in the Rat. Journal of neurotrauma 36, 2991-3004.
Windelborn, J.A., Mitchell, G.S., 2012. Glial activation in the spinal ventral horn caudal to cervical injury. Respiratory physiology & neurobiology 180, 61-68.
Winslow, C., Rozovsky, J., 2003. Effect of spinal cord injury on the respiratory system. Am J Phys Med Rehabil 82, 803-814.

Wu, J., Capelli, P., Bouvier, J., Goulding, M., Arber, S., Fortin, G., 2017. A V0 core neuronal circuit for inspiration. Nature communications 8, 544-544.
Wu M., V.S., Chen C., Lee K.Z. , 2019. 5-HT7 receptor inhibition enhances respiratory recovery following daily acute intermittent hypoxia in rats with chronic mid-cervical spinal cord contusion. Neurorehabilitation and Neural Repair, In press.
Zanella, S., Doi, A., Garcia, A.J., 3rd, Elsen, F., Kirsch, S., Wei, A.D., Ramirez, J.-M., 2014. When norepinephrine becomes a driver of breathing irregularities: how intermittent hypoxia fundamentally alters the modulatory response of the respiratory network. The Journal of neuroscience : the official journal of the Society for Neuroscience 34, 36-50.
Zholudeva, L.V., Karliner, J.S., Dougherty, K.J., Lane, M.A., 2017. Anatomical Recruitment of Spinal V2a Interneurons into Phrenic Motor Circuitry after High Cervical Spinal Cord Injury. Journal of neurotrauma 34, 3058-3065.

TABLES

Table 1. Animals weight evolution post-surgery

Table 2. Diaphragmatic EMG evaluation in eupneic vs mild asphyxia conditions in isoflurane-anesthetized mice.

FIGURES

Figure 1. Extent of injury following a C2 hemisection

A. Representative extend of injury for each animal at 1h post-injury (P.I.), 1d P.I., 3d P.I., 7d P.I., 15d P.I. and 30d P.I.. B. Extent of injury quantification in percentage compared to control spinal cord injury (SCI) 100%. The quantification has been made only in the ventral part where the phrenic motoneurons are located. There is no difference between the different groups (One-way ANOVA, $p = 0.248$). C. Representative spinal cord cross sections for each group at 1h P.I., 1d P.I., 3d P.I., 7d P.I., 15d P.I. and 30d P.I.. Scale bar: 800µm.

Figure 2. Diaphragm activity following a C2 hemisection

A. Representative traces of raw diaphragm EMG at 1h post-injury (P.I.), 1d P.I., 3d P.I., 7d P.I., 15d P.I. and 30d P.I.. B. Integrated diaphragm amplitude normalized to corresponding sham animal for 1h post-injury (P.I.), 1d P.I., 3d P.I., 7d P.I., 15d P.I. and 30d P.I. groups. a $p<0.05$ compared to corresponding Sham; b $p<0.05$ compared to 1h intact side group; # $p<0.05$ compared to 1d, 3d and 7d intact side groups; * $p<0.05$ intact side compared to injured side.

Figure 3. Diaphragm activity at 7d P.I. and during respiratory challenge

Integrated diaphragm amplitude for 1h P.I. (A), 1d P.I. (B), 3d P.I. (C), 7d P.I. (D), 15d P.I. (E) and 30d P.I. (F) groups (Sham and injured animals) in eupnea and during mild asphyxia. * $p<0.05$ mild asphyxia compared to eupnea (Paired t-test).

Figure 4. Inter-burst diaphragm recordings during EMG

A. Representative traces of raw inter-inspiratory bursts signals from diaphragm EMG at 1h post-injury (P.I.), 1d P.I., 3d P.I., 7d P.I., 15d P.I. and 30d P.I.. B. Amplitude of inter-burst diaphragm EMG signal normalized to corresponding sham animal for 1h P.I., 1d P.I., 3d P.I., 7d P.I., 15d P.I. and 30d P.I. groups. # $p<0.05$ compared to corresponding Sham; * $p<0.05$ compared to intact side; a $p<0.05$ compared to 3d P.I. injured side.

Figure 5. Power spectral density (PSD) of EMG recording between two inspiratory bursts following C2 hemisection

PSD between two inspiratory bursts for intact and injured sides at 1h (A), 1d (B), 3d and 7d (D) post-injury (P.I.). Data were gathered by boot of 100Hz and computed by using a 35 ms window. # $p<0.05$ compared to 1h, 7d, and 15d and 30d P.I. (data not shown); * $p<0.05$ compared to 1h, and 15d and 30d P.I. (data not shown); † $p<0.05$ compared to 1h and 30d P.I. (data not shown); ‡ $p<0.05$ compared to 1h, 3d, 7d, and 15d and 30d P.I. (data not shown); a $p< 0.05$ compared to corresponding injured side.

SUPPLEMENTARY DATA

Supplemental data 1. Power spectral density (PSD) of diaphragmatic EMG

PSD of inspiratory burst for Sham animal. Data were gathered by boot of 100Hz and computed from an entire respiratory burst.

Supplemental data 2. Power spectral density (PSD) of EMG recording between two inspiratory bursts following sham surgery.

PSD between two inspiratory bursts for intact and injured sides at 1h, 1d, 3d and 7d after sham surgery (all groups were pooled together). Data were gathered by boot of 100Hz and computed by using a 35 ms window.

Supplementary Table. Power spectral density (PSD) of EMG recording between two inspiratory bursts following C2 hemisection in isoflurane-anesthetized mice.

A.

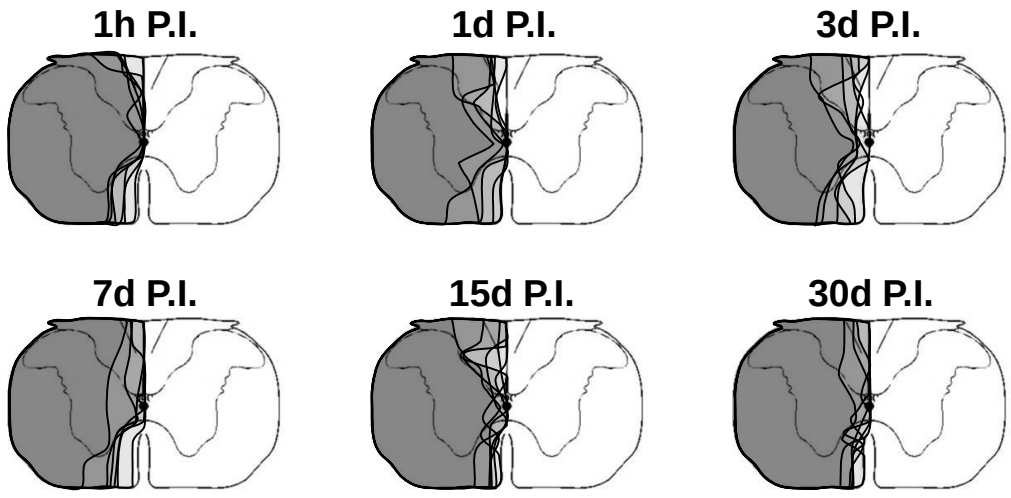
1h P.I.
1d P.I.
3d P.I.
7d P.I.
15d P.I.
30d P.I.

B.

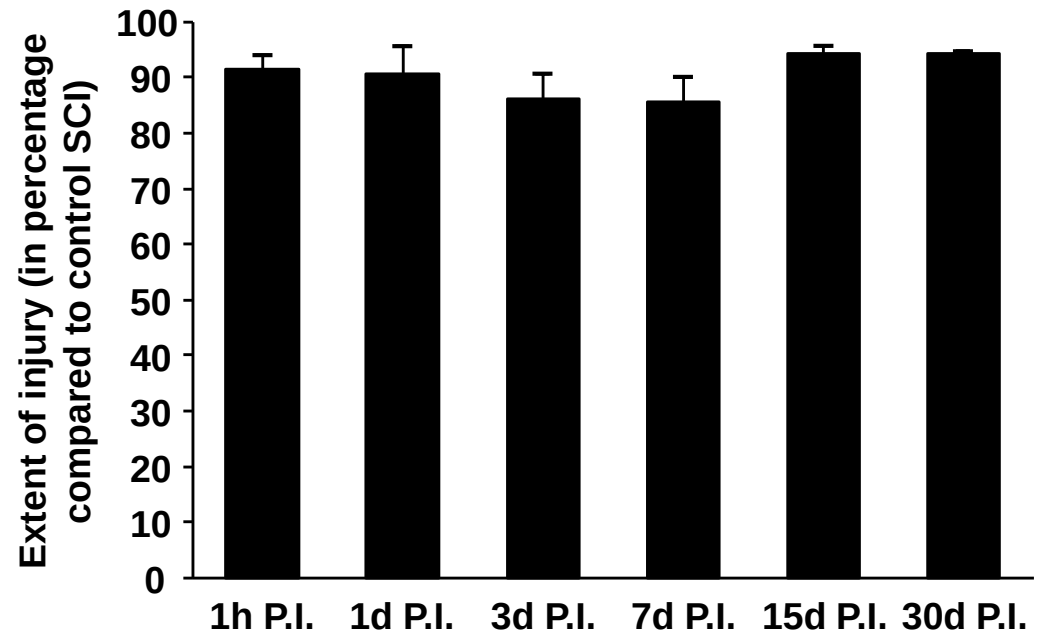
Extent of injury (in percentage compared to control SCI)
100
90
80
70
60
50
40
30
20
10
0
1h P.I.
1d P.I.
3d P.I.
7d P.I.
15d P.I.
30d P.I.

C.

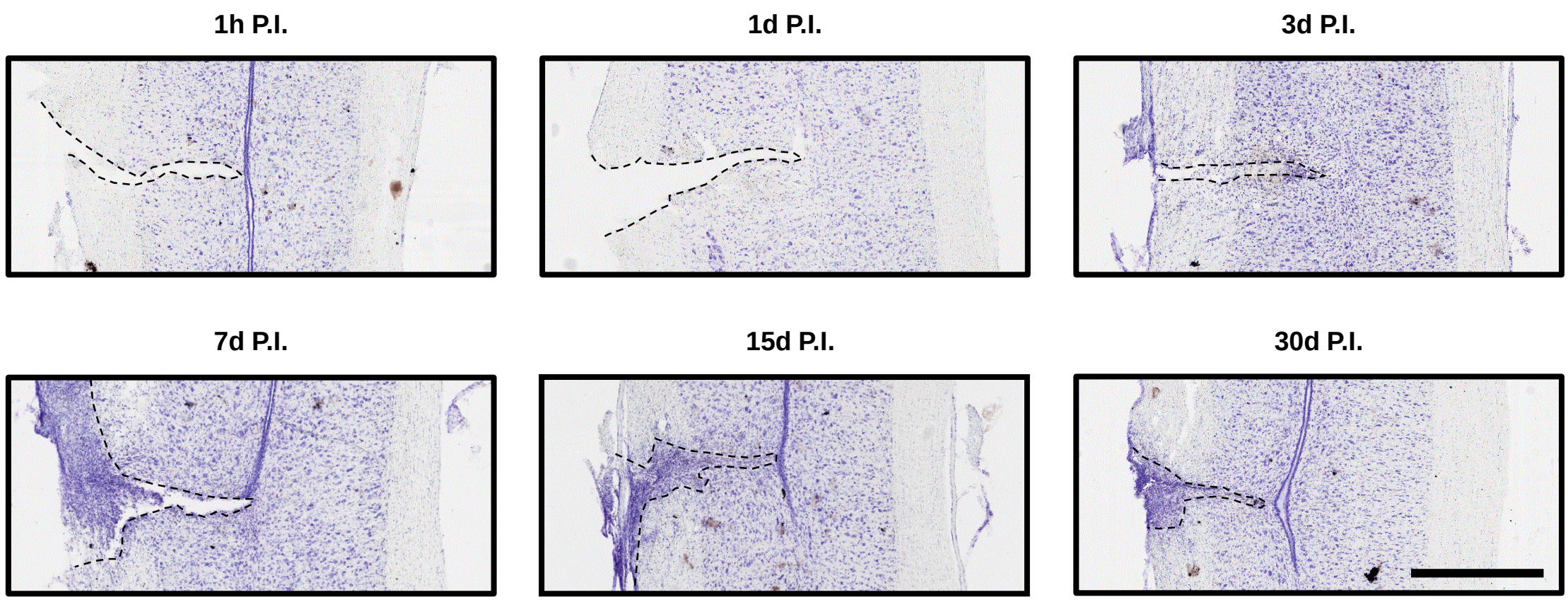
1h P.I.
1d P.I.
3d P.I.
7d P.I.
15d P.I.
30d P.I.

A.

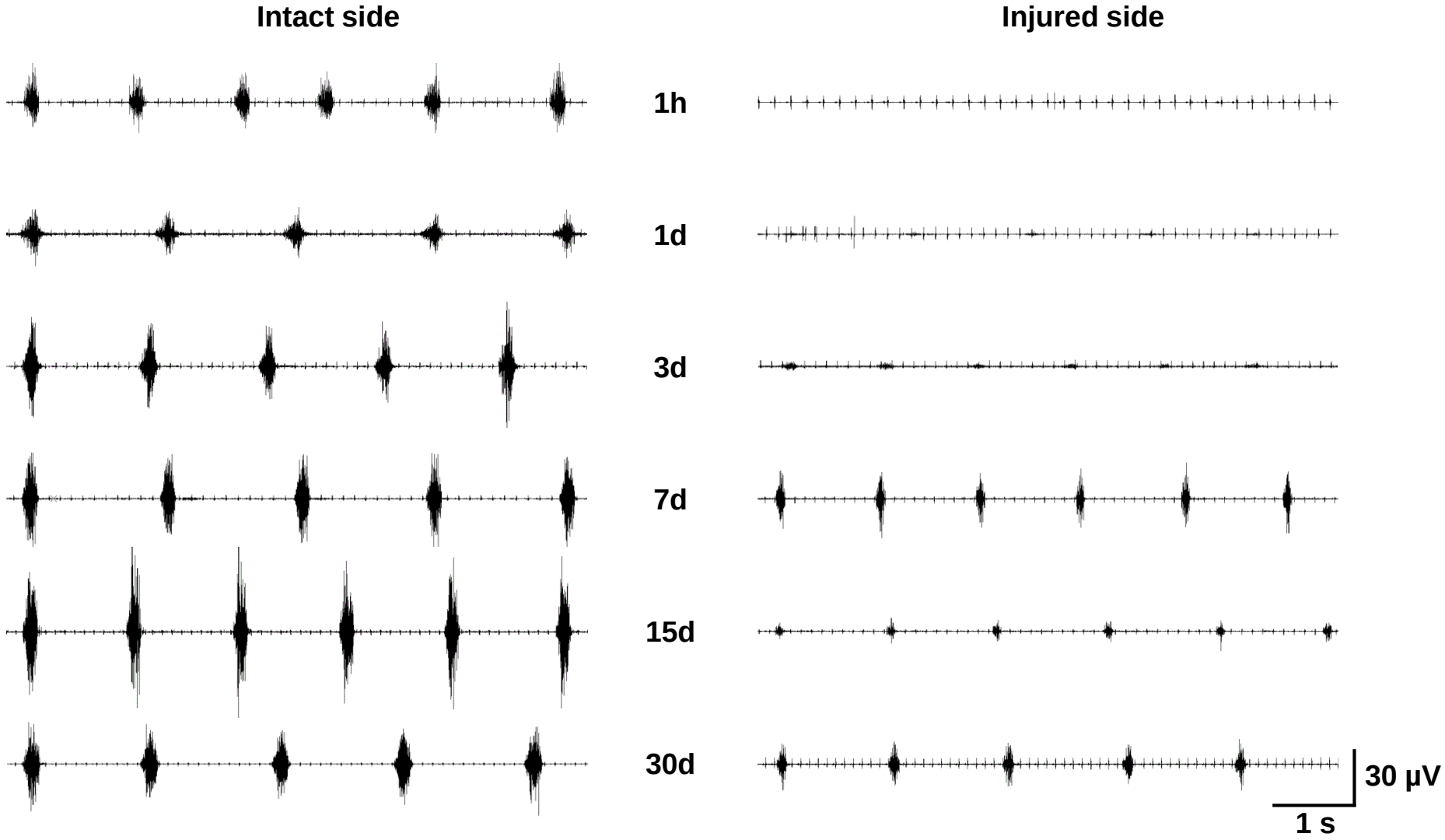
Intact side
Injured side
1h
1d
3d
7d
15d
30d
30 µV
1 s

B.

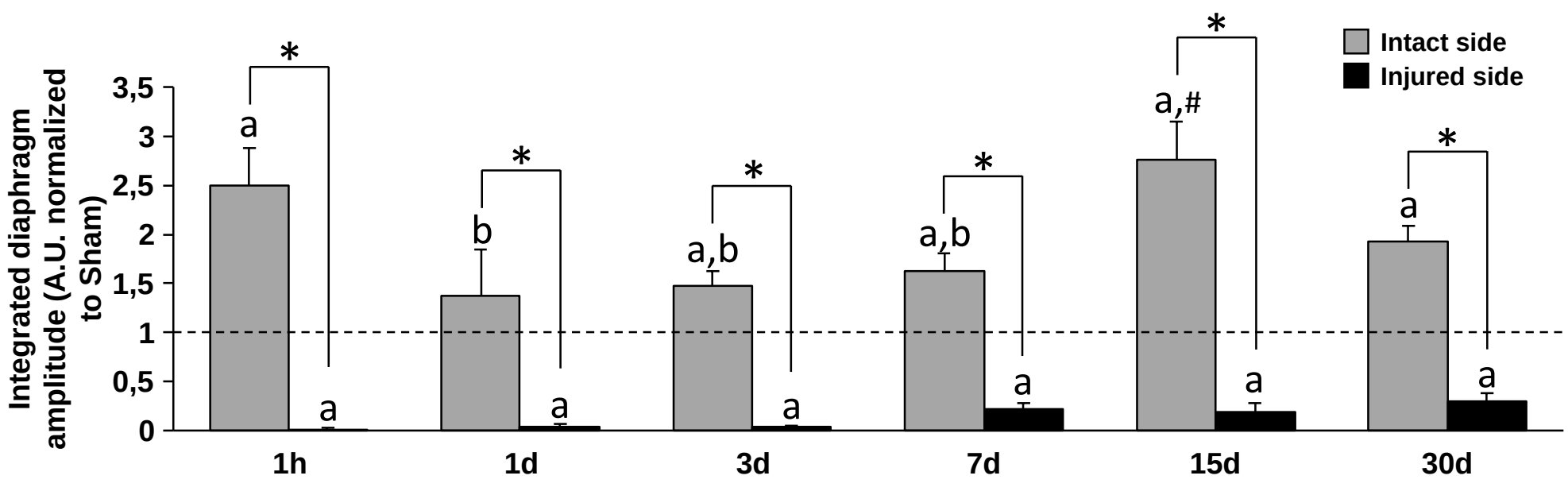
Integrated diaphragm amplitude (A.U. normalized to Sham)
3,5
3
2,5
2
1,5
1
0,5
0
Intact side
Injured side
*
a
b
a,b
a,#
1h
1d
3d
7d
15d
30d

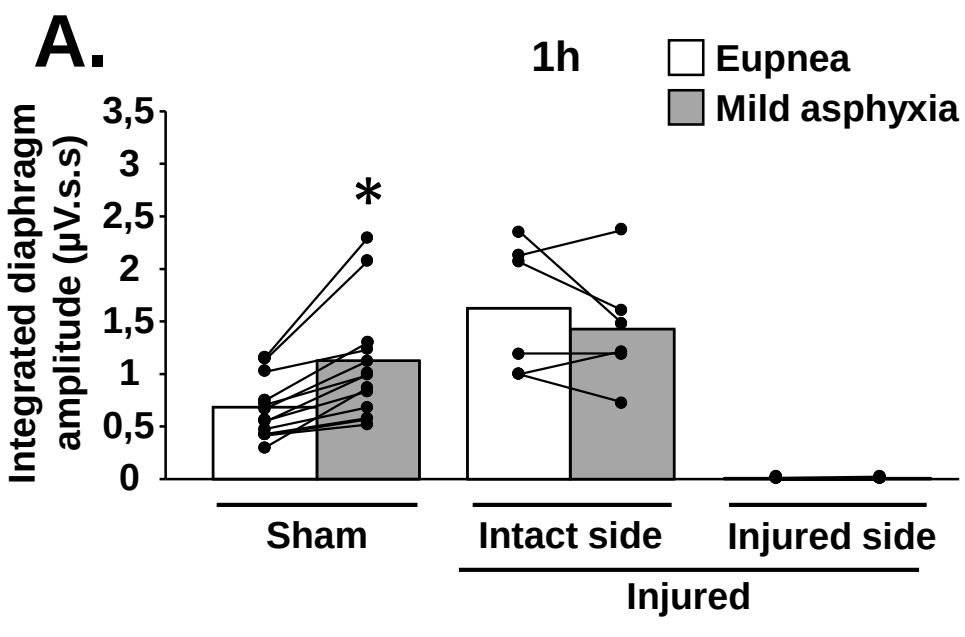
A.
1h
Eupnea
Mild asphyxia
Integrated diaphragm amplitude (µV.s.s)
3,5
3
2,5
2
1,5
1
0,5
0
*
Sham
Intact side
Injured side
Injured

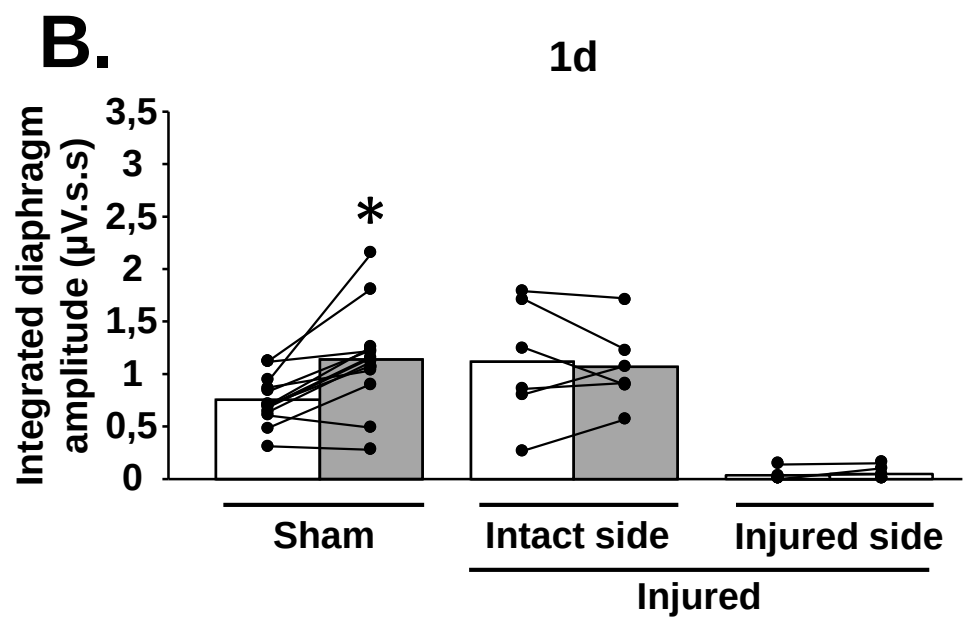
B.
1d
Integrated diaphragm amplitude (µV.s.s)
3,5
3
2,5
2
1,5
1
0,5
0
*
Sham
Intact side
Injured side
Injured

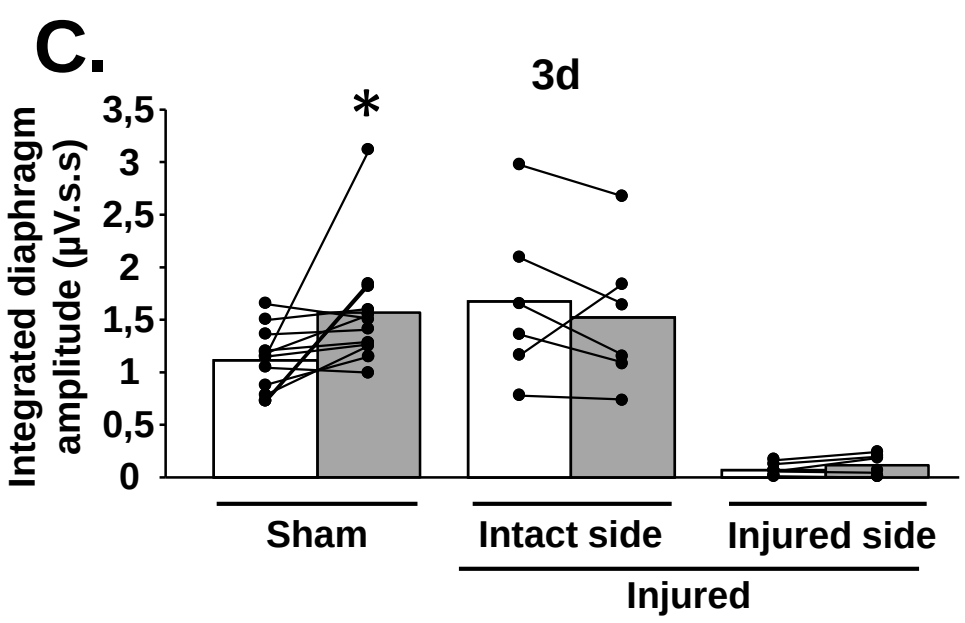
C.
3d
Integrated diaphragm amplitude (µV.s.s)
3,5
3
2,5
2
1,5
1
0,5
0
*
Sham
Intact side
Injured side
Injured

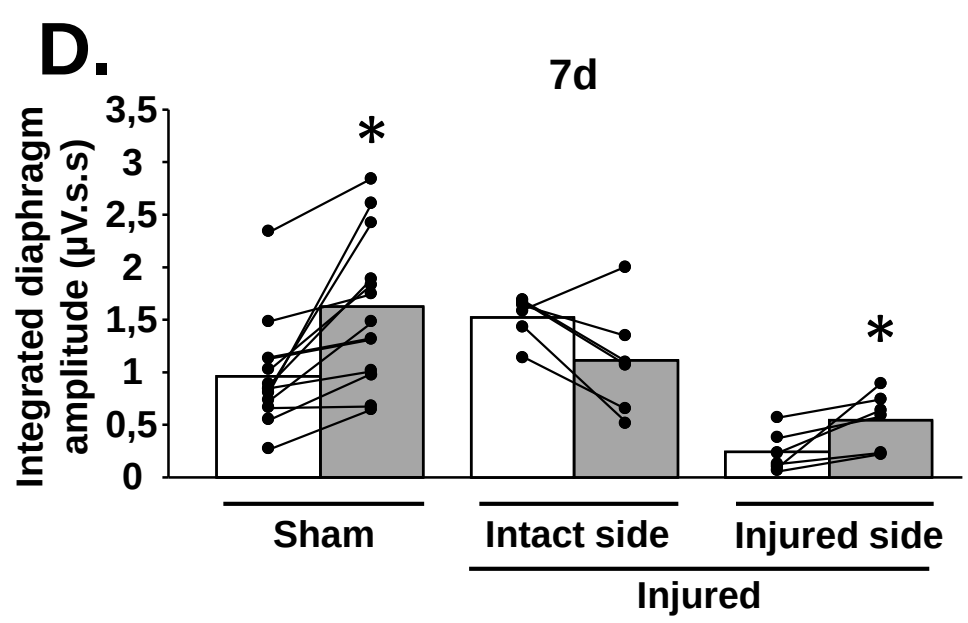
D.
7d
Integrated diaphragm amplitude (µV.s.s)
3,5
3
2,5
2
1,5
1
0,5
0
*
*
Sham
Intact side
Injured side
Injured

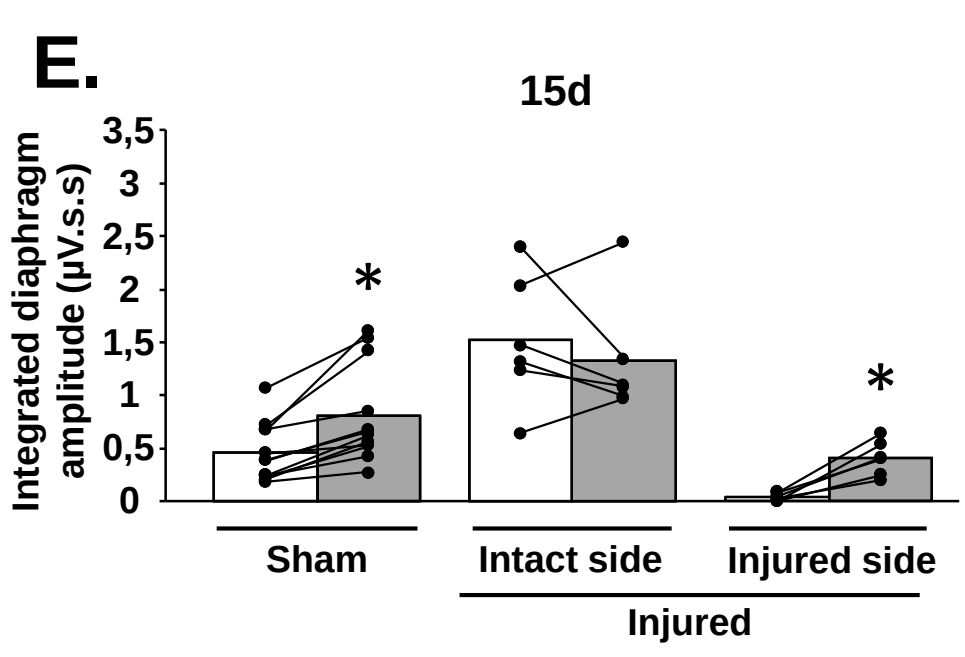
E.
15d
Integrated diaphragm amplitude (µV.s.s)
3,5
3
2,5
2
1,5
1
0,5
0
*
*
Sham
Intact side
Injured side
Injured

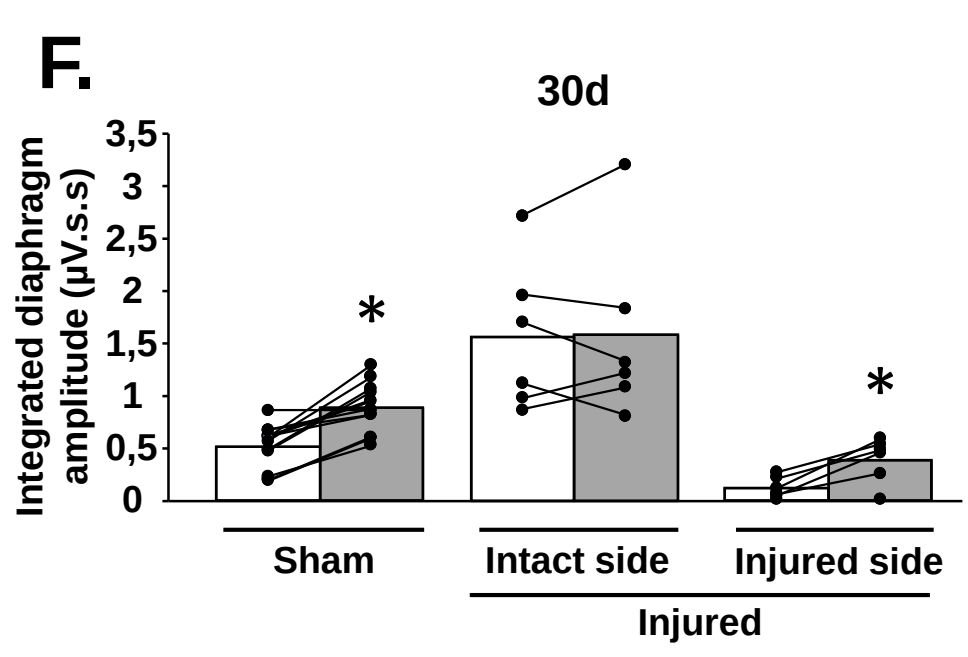
F.
30d
Integrated diaphragm amplitude (µV.s.s)
3,5
3
2,5
2
1,5
1
0,5
0
*
*
Sham
Intact side
Injured side
Injured

A.

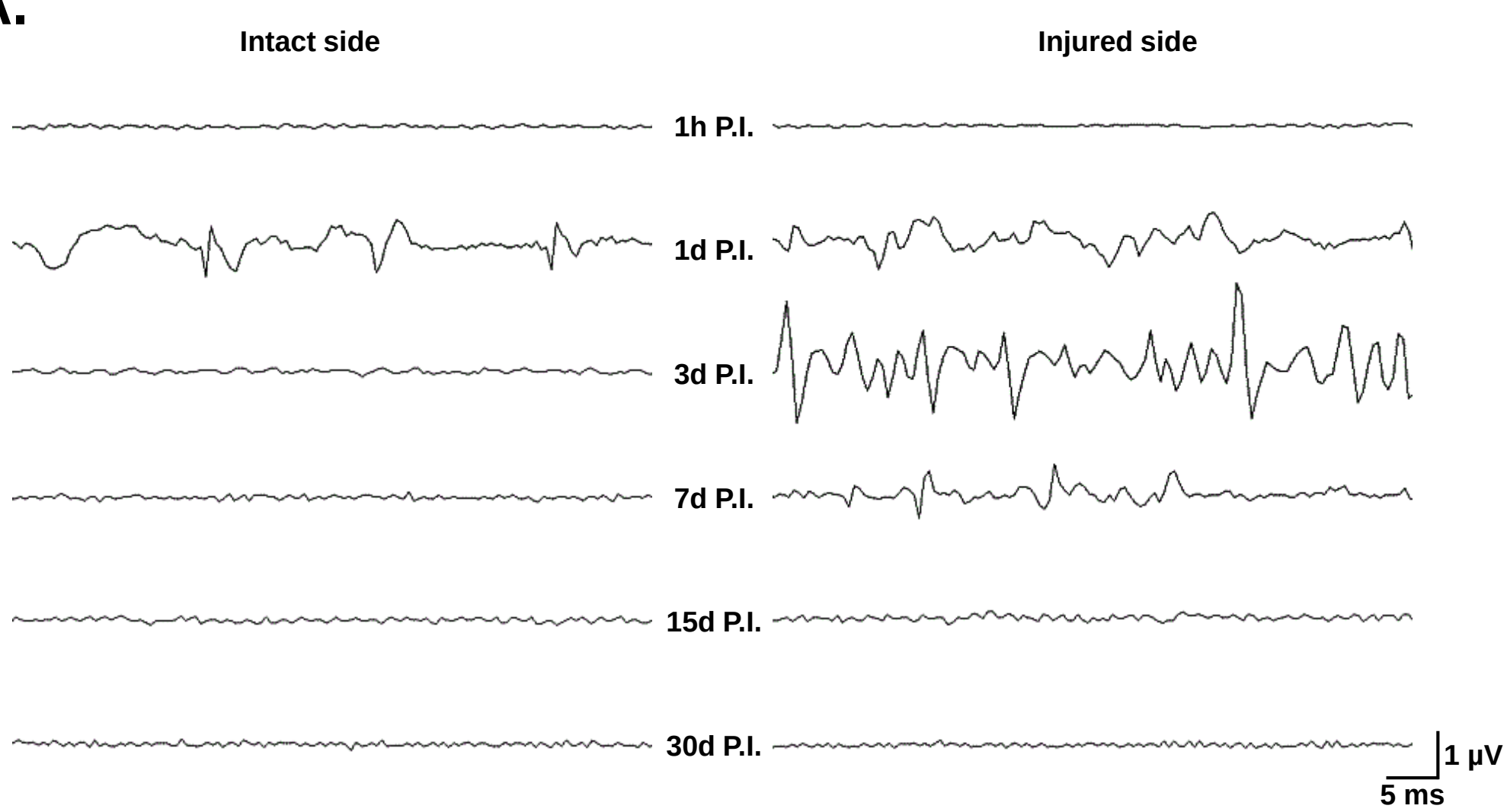
Intact side
Injured side
1h P.I.
1d P.I.
3d P.I.
7d P.I.
15d P.I.
30d P.I.
1 μV
5 ms

B.

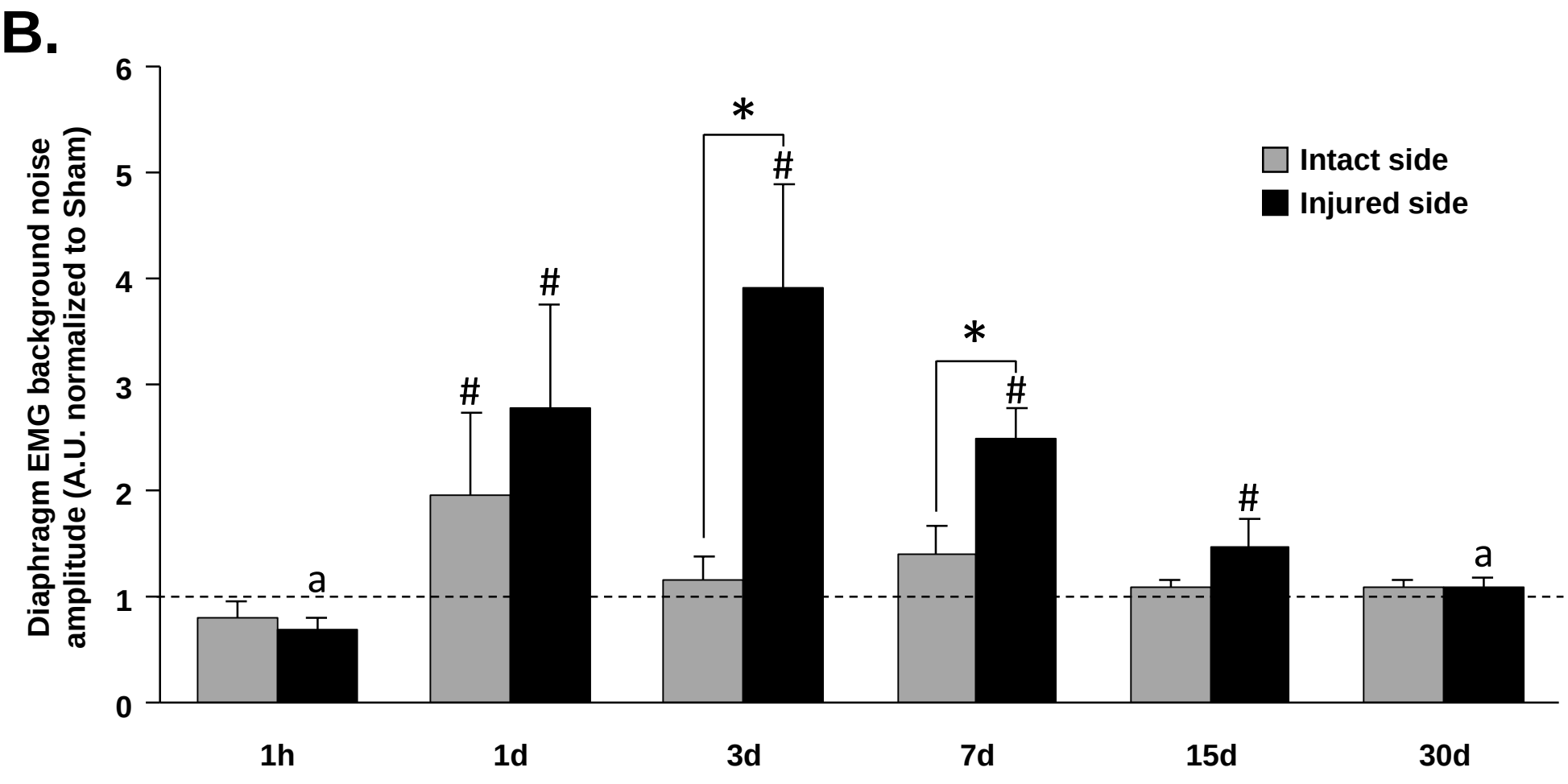
Diaphragm EMG background noise amplitude (A.U. normalized to Sham)
0
1
2
3
4
5
6
1h
1d
3d
7d
15d
30d
a
#
*
Intact side
Injured side

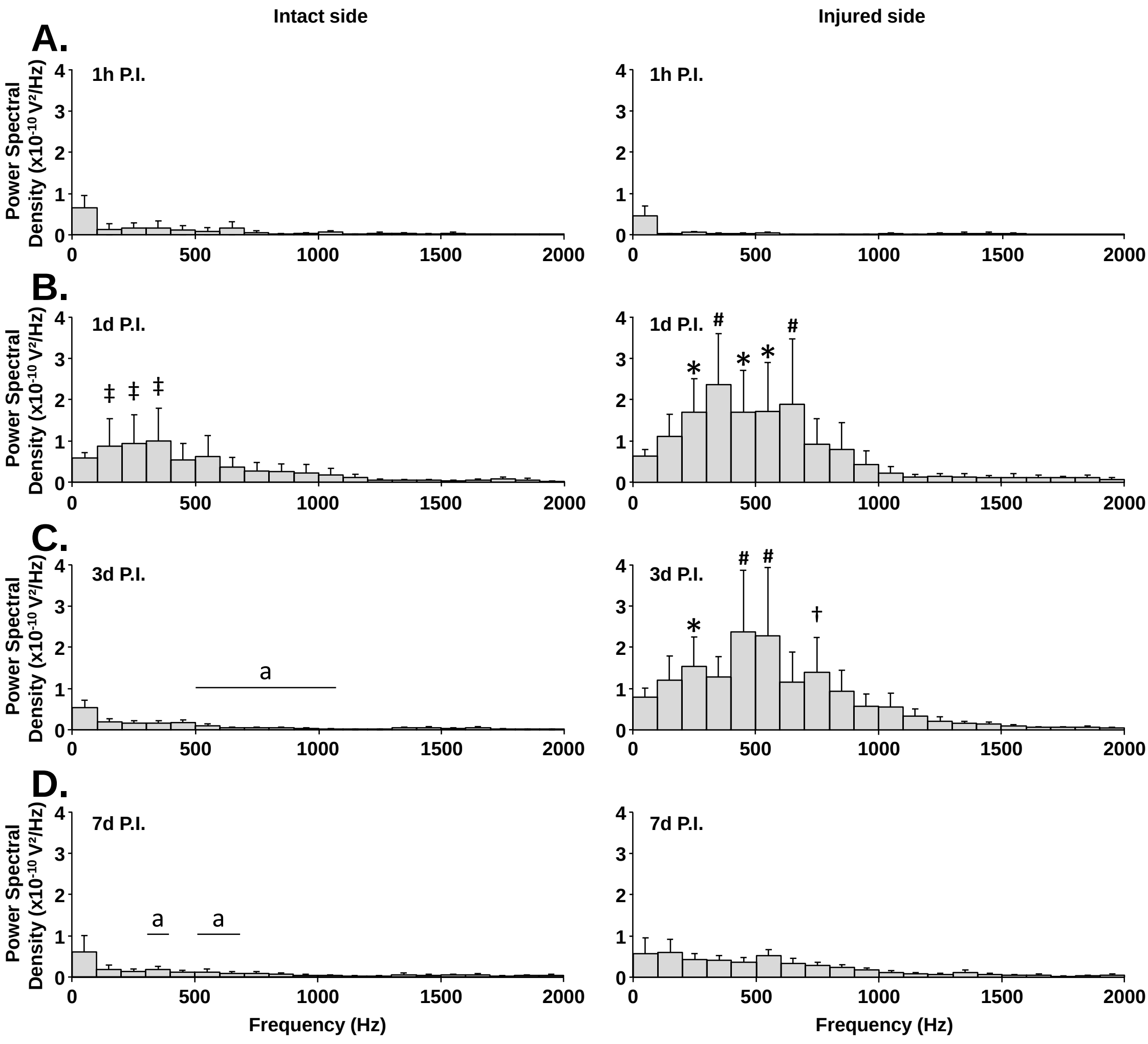
Intact side
Injured side
A.
1h P.I.
1h P.I.
B.
1d P.I.
1d P.I.
C.
3d P.I.
3d P.I.
a
D.
7d P.I.
7d P.I.
a
a
Power Spectral Density (x10-10 V²/Hz)
Frequency (Hz)
0
500
1000
1500
2000
1
2
3
4
‡
*
#
†

	Body weight (g)					
Group	**Initial weight**	**1d**	**3d**	**7d**	**15d**	**30d**
Sham	22.8 ± 0.5	21.1 ± 0.6	21.8 ± 0.9	22.2 ± 0.8	22.3 ± 1.5	25.3 ± 1.9
Injured	22.8 ± 0.6	21.9 ± 0.6	19.9 ± 0.7	21.5 ± 0.7	22.7 ± 1.4	23.3 ± 1.3

Table 1. Animals weight evolution post-surgery

Sham groups comparison: One-way ANOVA $p = 0.162$
Injured groups comparison: One-way ANOVA $p = 0.054$
Sham groups vs Injured groups comparisons: t-test, $p>0.05$

Group	Mean ± SEM	
	Eupnea (µV.s.s)	**Mild asphyxia (µV.s.s)**
Sham animals		
1h Sham	0.68 ± 0.09	1.13* ± 0.17
1d Sham	0.75 ± 0.07	1.14* ± 0.15
3d Sham	1.11 ± 0.09	1.57* ± 0.17
7d Sham	0.96 ± 0.16	1.62* ± 0.22
15d Sham	0.46 ± 0.08	0.81* ± 0.14
30d Sham	0.51 ± 0.06	0.88* ± 0.07
Injured (Intact side)		
1h P.I.	1.63 ± 0.28	1.43 ± 0.25
1d P.I.	1.12 ± 0.26	1.07 ± 0.17
3d P.I.	1.67 ± 0.35	1.53 ± 0.31
7d P.I.	1.53 ± 0.09	1.12 ± 0.24
15d P.I.	1.51 ± 0.28	1.32 ± 0.25
30d P.I.	1.56 ± 0.32	1.58 ± 0.39
Injured (Injured side)		
1h P.I.	$1.80x10^{-03}$ ± $1.97x10^{-03}$	$2.70x10^{-03}$ ± $2.96x10^{-03}$
1d P.I.	0.03 ± 0.03	0.05 ± 0.03
3d P.I.	0.07 ± 0.03	0.11 ± 0.05
7d P.I.	0.24 ± 0.09	0.55* ± 0.12
15d P.I.	0.04 ± 0.02	0.40* ± 0.07
30d P.I.	0.11 ± 0.05	0.38* ± 0.10

Table 2. Diaphragmatic EMG evaluation in eupneic vs mild asphyxia conditions in isoflurane-anesthetized mice.

* $p<0.05$ mild asphyxia compared to eupnea (Paired t-test)